

Determining Mars Parking Orbits that Ensure Tangential Periapsis Burns at Arrival and Departure

Prasun N. Desai*

NASA Langley Research Center, Hampton, Virginia 23666

and

James J. Buglia†

Flight Mechanics and Control Incorporated, Hampton, Virginia 23666

For a manned Mars mission, many previous interplanetary studies have arbitrarily assumed that the required parking orbit can be achieved with tangential periapsis burns at both Mars arrival and departure without considering the actual arrival and departure orbital geometries. As a consequence of this assumption, a misleading estimate of up to 50% of the initial low-Earth-orbit mass may result for the mission. In this paper, a method is presented that finds Mars parking orbits that allow tangential periapsis burns at both arrival and departure. This method accounts for the actual geometry at both arrival and departure between the hyperbolic asymptotes and the orbital plane, along with the precession effects caused by the oblateness of Mars. Thus, realistic ΔV values (and hence initial low-Earth-orbit masses) are obtained for these orbits. The results obtained from the present method compare very well with a trajectory integration program and require CPU times of only about 1 min. Therefore, because of its computational efficiency and accuracy, the present method would be an ideal tool to use in preliminary mission design, since it provides the opportunity to incorporate realistic Mars parking orbits effects.

Nomenclature

a	= semi-major axis of parking orbit, km
a_{hyp}	= semi-major axis of the approach or departure hyperbola, km
e	= eccentricity of parking orbit
e_{hyp}	= eccentricity of hyperbola
f_{∞}	= true anomaly at infinity, deg
h_p	= periapsis altitude, km
i	= inclination, deg
J_2	= second zonal harmonic of the Martian gravity field
k	= number of revolutions of the longitude of the ascending node
m	= number of revolutions of the argument of periapsis
n	= mean angular rate, deg/s
\hat{P}	= unit vector defining direction of periapsis
p	= semi-latus rectum, km
R_e	= equatorial radius of Mars, km
r_p	= periapsis radius, km
t	= stay time, s
v_{∞}	= hyperbolic excess velocity, km/s
α	= right ascension of the arrival or departure hyperbolic asymptote, deg
ΔV	= velocity increment, km/s
$\Delta\Omega$	= difference in longitude of ascending node, deg
$\Delta\omega$	= difference in argument of periapsis
δ	= declination of the arrival or departure hyperbolic asymptote, deg
δ_{max}	= maximum declination between the arrival and departure hyperbolic asymptotes, deg

θ	= true anomaly of parking orbit, deg
μ	= gravitational parameter of Mars, km ³ /s ²
ϕ	= angle between \hat{P} and the intersection of the arrival or departure hyperbolic
Ω	= longitude of the ascending node, deg
ω	= argument of periapsis, deg

Subscripts

arr	= arrival
dep	= departure

Introduction

EVER since the Apollo program, NASA has given serious consideration to a manned mission to Mars. Recent recommendations by President Bush, Sally Ride,¹ and the Synthesis Group² have further heightened interest in such a mission. As a result, many studies have produced preliminary guidelines on performing Mars missions for the early part of the next century. These guidelines have addressed most aspects of the mission, including propulsion options, crew sizes, trip times, mission opportunities, and radiation exposure limits.³⁻⁶ Considering these guidelines, parametric studies were performed to determine the minimum initial low-Earth-orbit (LEO) mass of the spacecraft proposed for these missions. However, accounting for every segment of the mission in these studies would require extensive analysis time. Therefore, in the past, many simplifying assumptions have been made. If some segments are neglected or not given serious consideration, an overly optimistic estimate of the initial LEO mass of the spacecraft may be made.

One mission segment frequently neglected is the Mars parking orbit, into which the Mars transfer vehicle would be inserted upon arrival. Many previous interplanetary studies arbitrarily assumed that a convenient parking orbit exists for the spacecraft, where tangential periapsis burns are possible at both Mars arrival and departure without taking into account the actual arrival and departure geometries between the respective hyperbolic asymptote and the parking orbit plane.^{5,7-9} Therefore, the validity of the arrival and departure velocity increments (ΔV values) obtained by these studies, based solely on orbital energy considerations (i.e., performing tangential

Presented as Paper 92-4582 at the AIAA Astrodynamics Conference, Hilton Head, SC, Aug. 10–12, 1992; received Oct. 5, 1992; revision received Dec. 23, 1992; accepted for publication Dec. 23, 1992. Copyright © 1993 by the American Institute of Aeronautics and Astronautics, Inc. No copyright is asserted in the United States under Title 17, U.S. Code. The U.S. Government has a royalty-free license to exercise all rights under the copyright claimed herein for Governmental purposes. All other rights are reserved by the copyright owner.

*Aerospace Engineer, Space Systems Division, Member AIAA.

†Aerospace Engineer.

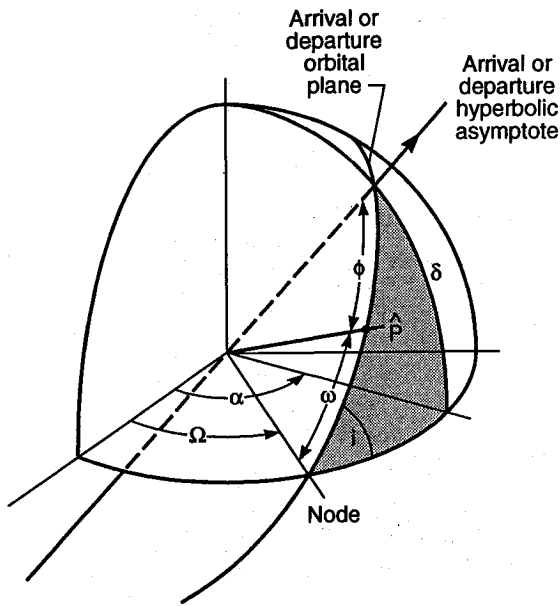


Fig. 1a Geometry between the hyperbolic asymptote and the orbital plane at arrival or departure.

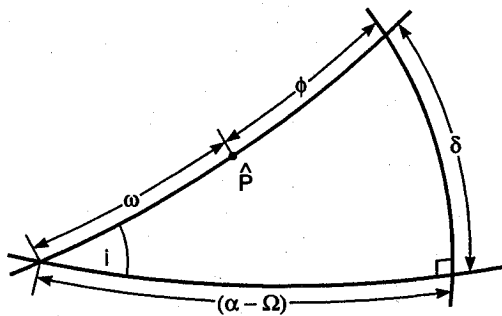


Fig. 1b Enlargement of shaded spherical triangle from Fig. 1a.

periapsis burns), is questionable. Additionally, a spherical Mars is assumed by these studies. Therefore, the parking orbit does not precess during the designated stay time, further diminishing the validity of the ΔV values. As a result, these simplifying assumptions may produce overly optimistic ΔV estimates and, hence, misleading initial LEO mission masses.

The recognition of the potential problems that might arise in taking the Mars parking orbit for granted was addressed in Ref. 10. That study showed that a penalty in the initial LEO mass as high as 50% can be realized if the arrival parking orbit plane is not properly selected. This penalty is mostly due to the out-of-plane ΔV that is required to align the departure velocity vector with the departure hyperbolic asymptote. This problem of avoiding the out-of-plane ΔV penalty was addressed by Ref. 11. In that study, the actual arrival and departure geometries were considered, along with the precession of the parking orbit, in determining an arrival orbital plane such that only in-plane burns are required at both arrival and departure. Thus, the arrival and departure ΔV values, and hence the initial LEO mass, can be significantly reduced. However, in obtaining the in-plane solutions, Ref. 11 only accounted for the precession of the longitude of the ascending node but not the line of apsides. As a result, only in-plane burns were possible using the method of Ref. 11. Therefore, a solution for determining parking orbits that use only tangential periapsis burns at both arrival and departure (as assumed by the previous studies) is still needed since this situation should result in the lowest ΔV requirement.

Thus, the subject of this paper is the development of a fast numerical method to determine the existence of Mars parking orbits that ensure tangential periapsis burns at both arrival and departure and take into account both the precession of the longitude of the ascending node and the line of apsides. Hence, the actual arrival and departure geometries, along with the precession of the parking orbit, are considered in obtaining the arrival and departure ΔV values. Therefore, a realistic estimate of the initial LEO mission mass can be obtained. Additionally, for a given interplanetary trajectory, this paper also shows that the inclination and eccentricity of the parking orbit are no longer independent parameters that can be selected arbitrarily, if tangential periapsis burns are used at arrival and departure. That is, the tangential periapsis burns requirement fixes the orbital geometry between the hyperbolic asymptotes and the parking orbit plane at arrival and departure. Consequently, only discrete values of the inclination and eccentricity of the parking orbit are possible that satisfy the interplanetary trajectory constraints. Hence, for a given interplanetary trajectory, only a limited number of parking orbits will exist that allow tangential periapsis burns at both arrival and departure.

Analysis

Since the arrival and departure hyperbolic asymptotes at Mars, along with the designated stay time, are known from the interplanetary trajectory, the following equations can be used to relate the geometry at Mars arrival or departure between the hyperbolic asymptote and the orbital plane (see Figs. 1a and 1b):

$$\sin(\alpha - \Omega) = \frac{\tan \delta}{\tan i} \quad (1)$$

$$\cos(\omega + \phi) = \cos(\alpha - \Omega) \cos \delta \quad (2)$$

$$\sin(\omega + \phi) = \frac{\sin \delta}{\sin i} \quad (3)$$

Equations (1-3) can be directly derived from Fig. 1b and spherical trigonometry, where α and δ are known from the interplanetary trajectory. In Figs. 1a and 1b, \hat{P} is a unit vector that defines the direction of periapsis, and ϕ is the angle between \hat{P} and the intersection of the hyperbolic asymptote, as

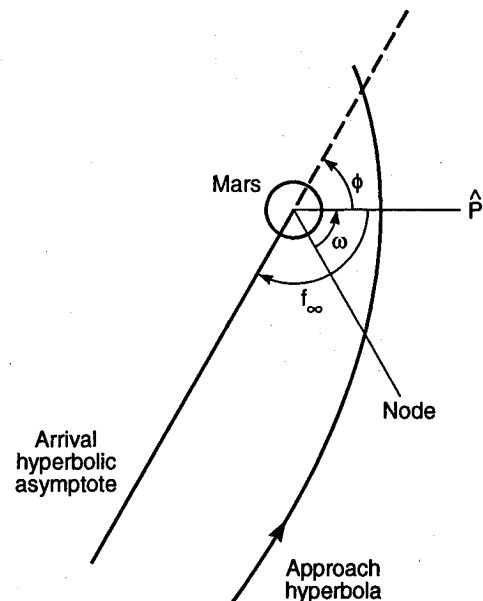


Fig. 2 Geometry between the arrival hyperbolic asymptote and the approach hyperbola.

it continues through the center of the planet (dashed line), and the orbital plane at arrival or departure.

Since tangential periapsis burns are performed at both Mars arrival and departure, the parking orbit and the hyperbola at arrival and departure share a common argument of periapsis ω . Therefore, if the arguments of periapsis of the approach and departure hyperbolas are found, the arguments of periapsis of the parking orbit at arrival and departure will be known. Additionally, the true anomaly θ of the parking orbit at arrival and departure is zero because tangential burns are performed at periapsis.

The argument of periapsis of the approach or departure hyperbola can be obtained by relating ϕ to its true anomaly at infinity (f_∞). Figures 2 and 3 show the relationship of the approach and departure hyperbolas with the arrival and departure hyperbolic asymptotes. Looking at these two figures, ϕ at Mars arrival and departure, respectively, is observed to be

$$\phi = 180 \text{ deg} - f_\infty \quad (4)$$

$$\phi = f_\infty \quad (5)$$

The true anomaly at infinity f_∞ of the approach or departure hyperbola can be calculated by relating it to its eccentricity e_{hyp} :

$$f_\infty = \cos^{-1} \left(\frac{-1}{e_{\text{hyp}}} \right) \quad (6)$$

where e_{hyp} can be obtained from the following equation defining the periapsis radius r_p of a hyperbola:

$$r_p = (R_e + h_p) = a_{\text{hyp}}(1 - e_{\text{hyp}}) \quad (7)$$

Eliminating a_{hyp} in Eq. (7) with

$$a_{\text{hyp}} = -\frac{\mu}{v_\infty^2} \quad (8)$$

and substituting into Eq. (6), f_∞ of the approach and departure hyperbola can be determined from the following equation,

$$f_\infty = \cos^{-1} \left[\frac{-\mu}{\mu + (R_e + h_p)v_\infty^2} \right] \quad (9)$$

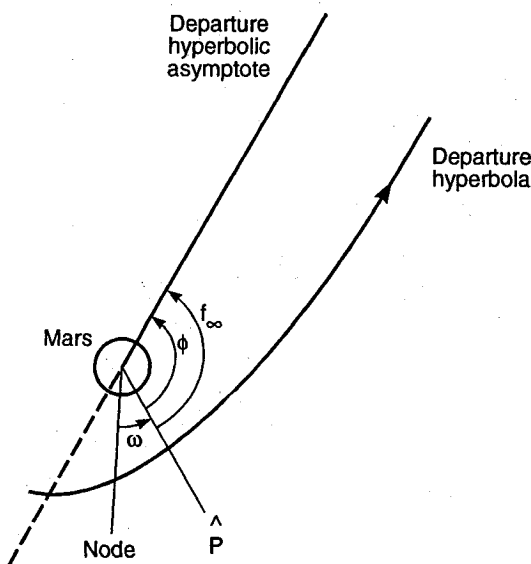


Fig. 3 Geometry between the departure hyperbolic asymptote and the departure hyperbola.

Table 1 Trajectory parameters and planetary constants

	Asymptote	
	Arrival	Departure
α , deg	253.9	212.66
δ , deg	-21.4	-12.5
v_∞ , km/s	5.441	3.873
Mars gravitational parameter μ , km/s		42,828.0
Mars J_2		1.9595×10^{-3}
Mars equatorial radius R_e , km		3,400.0

Table 2 Parking orbits obtained by the present method ($h_p = 500$ km)

i , deg	e	Ω_{arr} , deg	Ω_{dep} , deg	ω_{arr} , deg	ω_{dep} , deg	ΔV_{arr} , km/s	ΔV_{dep} , km/s
21.8	0.1102	355.4	359.0	185.1	100.7	3.690	2.588
27.4	0.0468	303.0	237.9	233.3	217.0	3.791	2.689
51.9	0.0960	271.9	22.7	258.1	81.0	3.712	2.611
56.1	0.1334	58.7	221.3	131.8	229.9	3.653	2.552
70.8	0.3953	261.9	217.1	263.0	231.7	3.267	2.166
75.0	0.3703	68.0	29.3	127.9	77.9	3.302	2.201
130.8	0.3451	93.8	201.7	134.5	228.4	3.338	2.237
133.4	0.0648	95.8	44.8	135.9	82.3	3.762	2.660
133.9	0.0496	231.9	200.4	255.3	227.5	3.786	2.685
135.4	0.2363	230.6	45.7	254.4	82.9	3.497	2.395

once a periapsis altitude h_p has been selected for the parking orbit. In Eq. (9), v_∞ is known from the interplanetary trajectory. Therefore, knowing f_∞ , ϕ can be determined and, hence, the argument of periapsis of the approach or departure hyperbola. Since tangential periapsis burns are performed, the orbital plans at arrival and departure have the same argument of periapsis as the respective hyperbolic orbit.

For a given inclination, the longitude of the ascending node of the arrival orbital plane can be determined from Eq. (1). Substituting this value into Eqs. (2) and (3), the sum of $\omega + \phi$ can be uniquely calculated because both the sine and the cosine functions are known. Once f_∞ is determined, ω of the arrival orbital plane can be found. Note that only the sine function is available for determining the longitude of the ascending node of the arrival orbital plane in Eq. (1). Therefore, the other quadrant solution for Ω must also be tried in Eqs. (2) and (3). As a result, there are two solutions for the arrival longitude of the ascending node and the argument of periapsis. Now, this procedure is repeated for the departure geometry (for the same value of inclination) to determine the argument of periapsis and the longitude of the ascending node of the departure orbital plane. Again, note that two values of the departure longitude of the ascending node and the argument of periapsis are obtained. Thus, the arrival and departure longitudes of the ascending node and arguments of periapsis of the orbital planes are known. Therefore, the difference in their values ($\Delta\Omega$ and $\Delta\omega$) sets up a criterion that must be satisfied by the precession rates of the parking orbits. That is, the eccentricity of the parking orbit must produce the precession required by the geometrical constraints imposed by the arrival and departure hyperbolic asymptotes. Knowing $\Delta\Omega$ and $\Delta\omega$, the equation relating the precession of these two quantities to the J_2 planetary oblateness expansion,¹²

$$\Delta\omega = \frac{3}{2} J_2 n t \left(\frac{R_e}{p} \right)^2 \left(2 - \frac{5}{2} \sin^2 i \right) \quad (10)$$

$$\Delta\Omega = -\frac{3}{2} J_2 n t \left(\frac{R_e}{p} \right)^2 \cos(i) \quad (11)$$

can be used to determine the value of the eccentricity that satisfies them during the designated stay time. In Eqs. (10) and

(11), t is known from the interplanetary trajectory. The semi-latus rectum p and the mean angular rate n can be defined as

$$p = a(1 - e^2) \quad (12)$$

$$n = \sqrt{\frac{\mu}{a^3}} \quad (13)$$

Substituting these into Eq. (10), and using the following transformation,

$$r_p = (R_e + h_p) = a(1 - e) \quad (14)$$

where r_p is the periapsis radius of the parking orbit, Eq. (10) can be expressed as

$$e^4 + \left(4 + \frac{c^2}{\Delta\omega^2}\right)e^3 + \left(6 - \frac{3c^2}{\Delta\omega^2}\right)e^2 + \left(4 + \frac{c^2}{\Delta\omega^2}\right)e + \left(1 - \frac{c^2}{\Delta\omega^2}\right) = 0 \quad (15)$$

where

$$c = \frac{3}{2} J_2 R_e^2 t \left(2 - \frac{5}{2} \sin^2 i\right) \sqrt{\frac{\mu}{(R_e + h_p)^7}} \quad (16)$$

Equation (15) is quartic in eccentricity only. Therefore, for a given inclination and periapsis altitude, the eccentricity that satisfies $\Delta\omega$ can be determined. A closed-form solution does exist for solving a quartic equation¹³; thus, the value of the eccentricity can be explicitly obtained. Note that the calculation of the eccentricity from the quartic solving algorithm in Ref. 13 should be performed in double precision. Also, note that the longitude of the ascending node and the argument of periapsis of the parking orbit could precess through more than one revolution during the specified stay time. Hence, a precession of $(k \times 360 \text{ deg}) + \Delta\Omega$ and $(m \times 360 \text{ deg}) + \Delta\omega$ could also be a solution and needs to be tried, where k and m are the number of revolutions of the longitude of the ascending node and the argument of periapsis of the parking orbit during the stay time, respectively.

Using the eccentricity obtained from Eq. (15), the precession of Ω (resulting from this eccentricity) can be found from Eq. (11). If this precession of Ω equals $\Delta\Omega$ (obtained from the geometrical constraints), then a tangential periapsis-to-periapsis transfer is possible for this inclination having the eccentricity obtained from Eq. (15). Once the eccentricity has been determined, the arrival and departure ΔV values at Mars can then be simply calculated from the difference in the velocities between the respective hyperbola and the parking orbit (because tangential periapsis burns are performed), where the velocities of the respective hyperbola and the parking orbit at arrival and departure can be determined from their energies. Finally, an iteration on the remaining values of inclination can be performed to obtain other eccentricities that may satisfy the geometry. Note that Eqs. (1) and (3) indicate that the inclination of the parking orbit is constrained by the declination of either the arrival or departure hyperbolic asymptote. Therefore, accounting for both the arrival and departure orbital geometries and using tangential periapsis burns, the inclination of the parking orbit must be within the following range:

$$|\delta_{\max}| \leq i \leq 180 \text{ deg} - |\delta_{\max}| \quad (17)$$

for the sine functions of Eqs. (1) and (3) to be defined. Also, the assumption of a constant inclination, eccentricity, and semi-major axis of the parking orbit over the length of the stay

time is consistent with the use of first-order theory in the gravitational model for Mars.

As mentioned, the quadrant in which Ω lies cannot be uniquely determined; therefore, there will be four combinations of $\Delta\Omega$ and $\Delta\omega$ for a particular geometry (i.e., for each value of inclination). As a result, there will be an eccentricity for each $\Delta\Omega/\Delta\omega$ combination. Equations (10) and (11) can be used to eliminate the combinations of $\Delta\Omega$ and $\Delta\omega$ that do not satisfy the geometrical constraints posed by the arrival and departure hyperbolic asymptotes. Dividing Eq. (10) by (11), the following relationship exists between the inclination of the parking orbit and $\Delta\Omega$ and $\Delta\omega$:

$$\frac{\Delta\omega}{\Delta\Omega} = \frac{2 - (5/2) \sin^2 i}{-\cos i} \quad (18)$$

Equation (18) can be used to screen the $\Delta\Omega/\Delta\omega$ combinations to produce the proper quadrant in which Ω lies at arrival and departure for each inclination. As a result, only one $\Delta\Omega/\Delta\omega$ combination will remain, and hence only one eccentricity will be produced. Note that, for a given inclination, there may be no combination of $\Delta\Omega$ and $\Delta\omega$ that satisfies Eq. (18). Therefore, a tangential periapsis-to-periapsis transfer will not be possible for that particular value of inclination or geometry.

Results and Discussion

To illustrate the method outlined in this paper, an opposition class Mars mission was arbitrarily selected from the set of opportunities presented in Ref. 5. The interplanetary trajectory, having a 60-day stay time at Mars, uses a Venus swingby on the outbound (Earth-Mars) leg and has a total trip time of 1.6 yr. The arrival and departure hyperbolic asymptotes at Mars are given in Table 1, along with the planetary constants that were used.

Table 2 shows the results from applying the present method, where a periapsis altitude h_p of 500 km was arbitrarily chosen for the parking orbit. As seen in Table 2, multiple tangential periapsis-to-periapsis transfer solutions are available with varying characteristics, where the inclination i , eccentricity e , and the arrival and departure longitudes of the ascending node Ω_{arr} and Ω_{dep} respectively, and arguments of periapsis ω_{arr} and ω_{dep} of the parking orbit are presented, respectively, along with the corresponding arrival and departure ΔV values, ΔV_{arr} and ΔV_{dep} . As seen, posigrade as well as retrograde parking orbits are possible with eccentricities ranging from near circu-

Table 3 Parking orbits obtained by POST ($h_p = 500 \text{ km}$)

i , deg	e	Ω_{arr} , deg	Ω_{dep} , deg	ω_{arr} , deg	ω_{dep} , deg	ΔV_{arr} , km/s	ΔV_{dep} , km/s
21.8	0.1132	354.7	359.1	185.8	100.6	3.686	2.584
27.5	0.0479	302.8	237.7	233.5	217.1	3.790	2.688
51.9	0.0951	271.9	22.6	258.1	80.9	3.713	2.611
56.2	0.1327	58.7	221.2	131.8	229.8	3.654	2.553
70.8	0.3934	261.8	217.0	263.0	231.9	3.268	2.167
75.0	0.3695	68.0	29.2	127.9	77.8	3.303	2.202
130.8	0.3459	93.8	201.5	134.5	228.4	3.337	2.236
133.4	0.0657	95.8	44.6	135.9	82.2	3.761	2.659
133.9	0.0495	231.9	200.0	255.3	227.4	3.786	2.685
135.4	0.2367	230.6	45.6	254.4	82.9	3.496	2.395

Table 4 Parking orbits obtained by the present method ($h_p = 250 \text{ km}$)

i , deg	e	Ω_{arr} , deg	Ω_{dep} , deg	ω_{arr} , deg	ω_{dep} , deg	ΔV_{arr} , km/s	ΔV_{dep} , km/s
62.9	0.2015	121.5	41.3	296.2	299.8	4.866	3.560
73.5	0.1898	312.8	261.0	86.5	31.7	4.885	3.578
136.7	0.0091	293.7	184.2	80.7	4.4	5.180	3.873
138.7	0.0740	292.6	138.8	79.8	330.1	5.071	3.764

lar to about 0.4 for this mission profile. Higher eccentricities for the parking orbits were not achievable for this mission profile because the stay time at Mars was not long enough to allow sufficient precession of the longitude of the ascending node and the argument of periapsis. However, in general, if a longer stay time is selected, higher energy parking orbits may be attainable. Note that the selection of an appropriate step size on the inclination range is critical in obtaining all valid solutions. A step size too large on the inclination range may miss some solutions, whereas a step size too small would reduce computational efficiency. Usually, a good step size to use on the inclination range is approximately 0.001 deg, as was the case for obtaining the results of the present paper. However, the step size will depend on the particular conditions being analyzed.

As seen from the results, there are only a limited number of parking orbits that allow tangential periapsis burns at both arrival and departure. This outcome is a consequence of constraining the periapsis burns to be tangential, which fixes the orbital geometry between the hyperbolic asymptotes and the parking orbit plane at arrival and departure. As a result, the arrival and departure orbital geometries dictate the necessary precession of the longitude of the ascending node and the argument of periapsis and hence, the inclination and eccentricity of the parking orbit. Therefore, if tangential periapsis burns are desired at both arrival and departure, the inclination and eccentricity of the parking orbit can no longer be independent parameters that are chosen arbitrarily.

The results of the present method were verified using the Program to Optimize Simulated Trajectories (POST),¹⁴ which numerically integrates the equations of motion. Table 3 shows the results obtained from POST. Comparing Tables 2 and 3, the inclination, eccentricity, and the arrival and departure longitudes of the ascending node and arguments of periapsis of the parking orbit are very close, within 1% for almost all cases. Additionally, the arrival and departure ΔV values between POST and the present method also agree very well, within 0.1% for all cases. The computation time required on a Silicon Graphics 360s computer for the present method is about 1 min of CPU time for all orbits shown in Table 2, whereas POST, on average, required about 6 h of CPU time for each orbit shown in Table 3. The computation times on POST were large because a good initial guess for the solution was not known to start the simulation. If the results obtained from the present method were used as initial guesses for the solutions, the computation time for POST could be reduced to about 2 h for each orbit. However, the two hours were still required because POST explicitly integrates the equations of motion.

Tables 4 and 5 show another comparison between the present method and POST for an opposition-class Mars mission obtained from Ref. 8. The interplanetary trajectory, having a 30-day stay time at Mars, uses a Venus swingby on the in-

bound (Mars-Earth) leg and has the arrival and departure hyperbolic asymptotes (with respect to Mars) as given in Table 6. For this example, a periapsis altitude of 250 km was arbitrarily chosen for the parking orbit. As seen, the results between the present method and POST compare well again, within 1% for almost all cases, with similar computation times as already stated. For this case, only four orbits were possible for performing tangential periapsis burns at both arrival and departure. This is a consequence of the short stay time at Mars. If more orbits are desired for a particular trajectory, a lower periapsis altitude should be selected since this condition will increase the precession of the longitude of the ascending node and the argument of periapsis as dictated by Eqs. (10) and (11), thus leading to more possible solutions. Moreover, in general, Mars missions (i.e., interplanetary trajectories) with longer stay times and/or with lower δ_{\max} values will produce more parking orbits that utilize tangential periapsis burns at both arrival and departure. This consequence is again a result of Eqs. (10) and (11), where a longer stay time and a lower δ_{\max} [hence, a lower inclination due to Eqs. (17), (1), and (3)] increase the precession of the longitude of the ascending node and the argument of periapsis.

The only limitation for the present method is that the gravitational model of Mars only includes the second zonal harmonic term J_2 . This approach was selected in an effort to efficiently determine the precession of the longitude of the ascending node and the argument of periapsis of the parking orbit. As a result, any perturbations to the parking orbit caused by other gravitational coefficients, atmospheric drag, or solar radiation pressure are not considered. However, for preliminary mission design, the J_2 term is adequate in obtaining reliable results, since it is the dominant gravitational coefficient for Mars.

With the use of the present method, a drastic reduction in the computation time can be achieved, without losing much accuracy in the results. Therefore, the present method would be an ideal tool for preliminary mission design, where it could be incorporated as a subroutine in a patched conic interplanetary trajectory code (such as SWISTO¹⁵ or MULIMP¹⁶) due to its low computation requirements. As a result, actual arrival and departure ΔV values can be obtained for parking orbits that use tangential periapsis burns at both Mars arrival and departure. Thus, a realistic initial LEO mass can be determined for each interplanetary trajectory, instead of arbitrarily assuming ideal conditions for Mars insertion and departure as is done currently in many interplanetary studies.

Summary

In this paper, a method is presented that finds Mars parking orbits that allow tangential periapsis burns at both arrival and departure. In obtaining these orbits, the present method considers the actual geometry between the hyperbolic asymptotes and the orbital plane at both arrival and departure, along with the precession effects caused by the oblateness of Mars. As a result, realistic arrival and departure ΔV values (and hence initial low-Earth-orbit masses) can be obtained. The results of the present method were verified using the Program to Optimize Simulated Trajectories (POST), a trajectory integration code; the differences in the inclination, eccentricity, and the arrival and departure longitudes of the ascending node and arguments of periapsis of the parking orbits were within 1% for almost all cases. Additionally, the arrival and departure ΔV values were within 0.1%. The computation time required to obtain the results using the present method were about 1 min of CPU time, whereas POST required hours of CPU time for each orbit. Therefore, due to the computational efficiency, the present method would be ideal for preliminary mission design, where it could be incorporated into a patched conic interplanetary trajectory code. As a result, actual arrival and departure ΔV values and, hence, a realistic initial low-Earth-orbit mass, can be calculated for each interplanetary trajectory.

Table 5 Parking orbits obtained by POST ($h_p = 250$ km)

i , deg	e	Ω_{arr} , deg	Ω_{dep} , deg	ω_{arr} , deg	ω_{dep} , deg	ΔV_{arr} , km/s	ΔV_{dep} , km/s
62.8	0.2004	121.5	41.4	296.2	299.9	4.867	3.564
73.5	0.1876	312.8	261.1	86.5	31.8	4.886	3.577
136.8	0.0095	293.7	184.2	80.6	4.4	5.179	3.871
138.8	0.0744	292.6	138.9	79.8	330.1	5.070	3.762

Table 6 Trajectory parameters for the second comparison

	Asymptote	
	Arrival	Departure
α , deg	128.7	66.7
δ , deg	13.7	39.9
v_{∞} , km/s	7.131	5.480

References

- ¹Ride, S. K., "Leadership and Americas Future in Space—A Report to the Administrator," NASA, Aug. 1987.
- ²Stafford, T. P., "America at the Threshold," America's Space Exploration Initiative, Report of the Synthesis Group, U.S. Government Printing Office, Washington, DC, May 1991.
- ³Braun, R. D., and Blersch, D. J., "Propulsive Options for a Manned Mars Transportation System," *Journal of Spacecraft and Rockets*, Vol. 28, No. 1, 1991, pp. 85-92.
- ⁴Santy, P. A., "Manned Mars Mission Crew Factors," Manned Mars Mission Conference, NASA TM 89320, June 1986.
- ⁵Braun, R. D., "The Influence of Interplanetary Trajectory Options on a Chemically Propelled Manned Mars Vehicle," *Journal of Astronautical Sciences*, Vol. 38, No. 3, pp. 289-310.
- ⁶Nachtwey, D. S., "Manned Mars Mission Radiation Environment and Radiobiology," Manned Mars Mission Conference, NASA TM 89320, June 1986.
- ⁷Striepe, S. A., "Interplanetary Trajectory Optimization of Mars Aerobraking Mission with Constrained Atmospheric Entry Velocities," American Astronomical Society, AAS Paper 91-421, Aug. 1991.
- ⁸Soldner, J. K., "Round-Trip Mars Trajectories: New Variation on Classic Mission Profiles," AIAA Paper 90-2932, Aug. 1990.
- ⁹Young, A. C., Mulqueen, J. A., and Skinner, J. E., "Mars Exploration Venus Swingby and Conjunction Class Mission Modes Time

Period 2000-2045," NASA TM-864777, Aug. 1984.

¹⁰Desai, P. N., and Braun, R. D., "Mars Parking Orbit Selection," *Journal of Astronautical Sciences*, Vol. 39, No. 4, 1991, pp. 447-467.

¹¹Desai, P. N., and Buglia, J. J., "Determining Mars Parking Orbits which Ensure In-Plane Arrival and Departure Burns," *Journal of Astronautical Sciences*, Vol. 40, No. 3, 1992, pp. 335-349.

¹²Roy, A. E., *Orbital Motion*, 2nd ed., Adam Hilger Ltd., Bristol, England, UK, 1982, pp. 283-290.

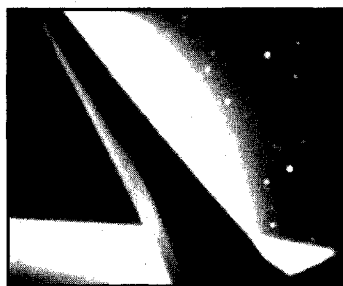
¹³Escobal, P. R., *Methods of Orbit Determination*, Krieger Publishing Co., Malabar, FL, 1976, pp. 430-434.

¹⁴Brauer, G. L., Cornick, D. E., and Stevenson, R., "Capabilities and Applications of the Program to Optimize Simulated Trajectories (POST)," NASA CR-2770, Feb. 1977.

¹⁵Mead, C. W., and Fox, M. F., "Optimization of Ephemerical Parameters for Minimum Propellant Requirements on Multiplanet Roundtrip Swingby-Stopover Missions (SWISTO)," Lockheed Missiles and Space Co., TM 54/30-189, LMSC/HREC A791436, Huntsville, AL, May 1968.

¹⁶Friedlander, A. L., "Multi-Impulse Trajectory and Mass Optimize Program (MULIMP)," Science Applications, Inc., Rept. SAI 1-120-383-T4, Rolling Meadows, IL, April 1975.

Michael E. Tauber
Associate Editor



The Space Environment: Implications for Spacecraft Design

September 13-14, 1993 Washington, DC

Learn how the space environment interacts with spacecraft and their subsystems and how these interactions should drive spacecraft design. Find out what parameters describe the space environment, how the space environment physically interacts with space systems, and what methods to use to estimate the magnitude of the interactions.

The focus of this two-day short course is on problem-solving techniques and design guidelines. You will learn how the various interactions are related to specific orbital environments and engineering design parameters.



American Institute of
Aeronautics and Astronautics

FAX or call David Owens, Phone 202/646-7447, FAX 202/646-7508 for more information.